

GAS REACTIONS OF CARBONS AND GRAPHITES

P. L. WALKER, JR.

Department of Fuel Technology, The Pennsylvania State University, University Park, Pennsylvania

(Manuscript received September 3, 1955)

The following properties of carbons have been investigated: quantitative and qualitative ash analyses, interlayer spacing, average crystallite size, surface area, pore volume distribution in pores from 20 Å to 130,000 Å radius, resistivity, helium density, apparent density, porosity, and effective diffusion coefficients of hydrogen-nitrogen through the carbons. The determination of these properties and their possible relation to the gas reactions of carbons and graphites are discussed.

The research on gas reactions of carbons and graphites has essentially broken down into two main categories—one, the attempted correlation of the chemical and physical properties of carbons with their gasification rates and two, the changes in these properties upon gasification of the carbon.

When our research on gas reactions of carbons was first started, it was apparent that the majority of prior research was related to the kinetics of reactions of gases with poorly defined carbonaceous materials. We felt that if a fundamental understanding of gas reactions of carbon was to be forthcoming the carbonaceous material being gasified had to be thoroughly described. Therefore, in our studies we have made a conscientious attempt to describe, by a number of parameters, the properties of our carbons. This paper is primarily a discussion of the techniques which we have been using to describe such carbons.

Figure 1 is a drawing of the reaction rate apparatus. The reactor is a ceramic tube placed vertically in a Globar furnace. In the bottom of the reactor, is a porcelain pier with a "v-notch" cut in its top. Carbon samples two inches in length and $\frac{1}{2}$ inch in diameter, with a porcelain cone attached to the base of the sample, are supported on the

ceramic pier. To the top of the carbon sample, is attached a $\frac{1}{8}$ inch long ceramic rod which in turn is connected to a Roller-Smith balance. During weighing, the carbon sample is raised off the ceramic pier; at all other times it is centered in the furnace resting on the pier. Reaction rates are determined by weight readings at necessary intervals.

Figure 2 shows a picture of some typical reaction rate curves for the gasification of a 10-gram sample of graphitized carbon. The reaction rate curves essentially break down into three main regions—an increasing reaction rate up to about 5% burn-off, a period of constant rate from about 5% to 30% burn-off, and a period of continually decreasing rate above 30% burn-off. The change in rate is paralleled, at least qualitatively, by the change in total surface area of the carbon during gasification. That is, during the early stages of gasification there is a marked increase in surface area, followed by a period in which the surface area is essentially constant. Past 30% burn-off the surface area continually decreases. In the majority of the gasification studies to date, the carbon-carbon dioxide reaction has been used. This is probably the simplest gasification reaction since there is only one product formed—carbon dioxide. Secondly,

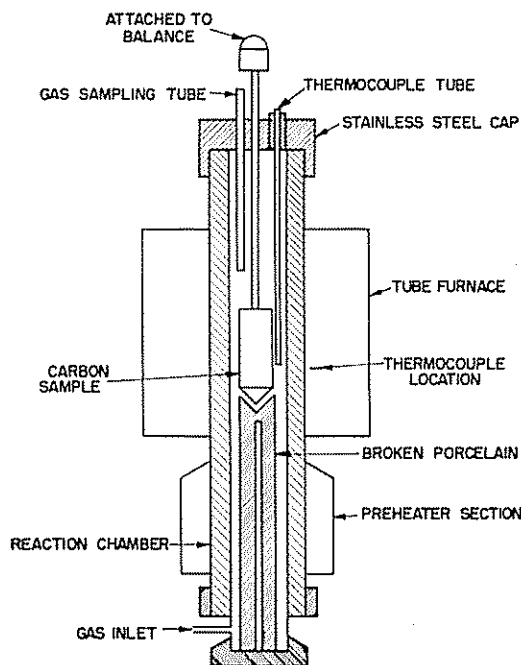


FIG. 1. Cross section of reaction chamber

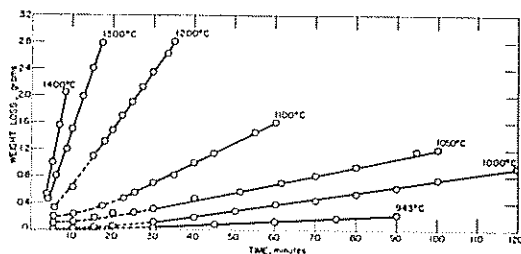


FIG. 2. Reaction curves for graphite at various temperatures.

since the reaction is endothermic, the reaction temperature is easily controlled.

Figure 3 presents an idealized picture of a carbon particle, which is the building block of the carbon rods reacted. The particle is composed of an inner core of filler material, usually petroleum coke, surrounded by a layer of binder material, usually coal tar pitch. Both the filler and binder materials are composed of a number of crystallites, the number of crystallites per particle usually being related to the graphitic character of the carbon. In the drawing, the

size of the binder crystallites is shown to be somewhat smaller than that of the filler crystallites. This is usually the case in both the raw and graphitized state. These particles then are bound together to form the rods, which are reacted as described above.

Table I presents a list of the techniques and parameters which we have used to study carbons. It should be pointed out that there are certainly other parameters and techniques which can also, in the future, prove of importance in the study of carbons.

We can first consider briefly emission spectroscopy and mass spectroscopy. Emission spectroscopy is used to determine both qualitative and quantitative analyses of

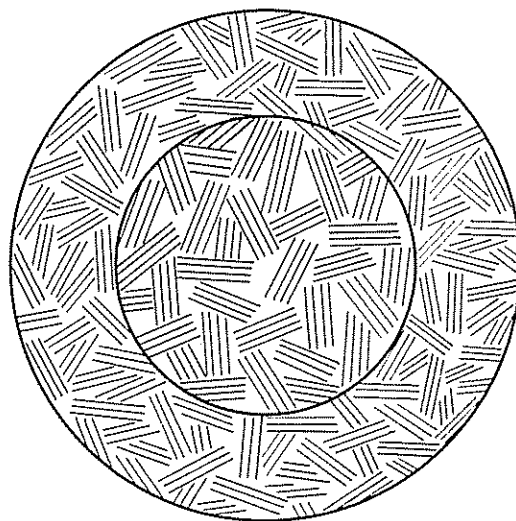


FIG. 3. Typical carbon particle composing carbon electrode.

TABLE I

Techniques and Parameters Used to Study Carbons

X-ray diffraction	Apparent density
Gas adsorption	Gas diffusion rates through carbons
Mercury porosimetry	Chemisorption
Resistivity	Emission spectroscopy
Helium density	Mass spectroscopy

TABLE II
Crystallite Size and *d*-Spacings of Carbons

	<i>d</i> -Spacing	\bar{L}_c	\bar{L}_a
	Å	Å	Å
Graphitized carbon A	3.360	900	1100
Graphitized carbon B	3.357	1200	∞
Lampblack.....	3.484	28	59
Carbon A.....	3.456	33	55
Carbon B.....	—	—	—
Carbon C.....	3.450	41	62

the mineral impurities in carbons. It is well known that these mineral impurities catalyze the gas reaction rates of carbons and; therefore, in any attempted correlation of these rates with properties of carbons, this information must be available.

The use of mass spectroscopy for the understanding of gas reactions is forthcoming in our laboratory. We plan to analyze qualitatively and quantitatively the gases which come off of graphite at high temperatures. From this information, we hope to better clarify the number and nature of active sites in graphite and correlate this with gasification rates.

Table II presents some typical data on carbons determined by x-ray diffraction. Two useful parameters which are determined by x-ray diffraction are interlayer spacing and average crystallite size of the carbon. With the use of the Franklin correlation¹, which says that pure graphite has a spacing of 3.354 Å and that amorphous carbon has a spacing of at least 3.44 Å, we are able from the *d*-spacing value to place the graphitic character of the carbon on at least a semi-quantitative basis. Table II presents data on six carbons, five of which have petroleum coke as the filler, all of which have coal tar pitch as the binder. It is seen that the two graphitized carbons have interlayer spacings approaching closely the Franklin value for 100% graphite. On the other hand, the lampblack and carbons have spac-

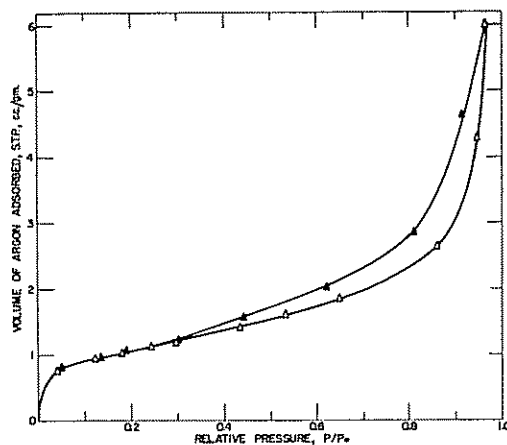


FIG. 4. Isotherms of argon on gas baked carbon

ings greater than 3.44 Å, or are completely amorphous. Crystallite size data, both \bar{L}_c , the height of the crystallite, and \bar{L}_a , the diameter of the crystallite, are given. For a well-graphitized carbon the crystallite size is usually greater than 500 Å. On the other hand, for an amorphous material the crystallite size is usually less than 100 Å.

Figure 4 presents a typical type II isotherm² for the adsorption of argon on a gas-baked carbon at liquid nitrogen temperatures. The isotherm essentially breaks down into three regions. At very low relative pressure, there is a sharp increase in volume due to the adsorption of a monolayer on the surface. There is then followed a period of multilayer adsorption over which there is only a slight increase in adsorption volume with increase in relative pressure. At high relative pressures, there is a sharp increase in adsorption volume because of capillary condensation. The isotherm up to a relative pressure of 0.3 can be used in conjunction with the BET equation to determine the surface area of the carbon. The upper portion of the isotherm, over the range of hysteresis in this case, can be used in conjunction with the Kelvin equation³ to de-

² H. E. Ries, Jr., *Catalysis* (Reinhold Publishing Co., New York, 1954) p. 12.

³ Conway Pierce, *J. Phys. Chem.*, **57**, 149 (1953).

¹ R. E. Franklin *Acta. Cryst.*, **4**, 253 (1951).

termine the distribution of pore volume over the pore radius range 20 to 350 Å.

Table III presents some typical surface area data for the six carbons (each originally weighing approximately 10 grams) previously discussed. Surface area data on the unreacted carbon, carbon after 10% burn-off at 900°C, and after 20% burn-off at 1100°C are presented. A considerable variation in the surface area of the unreacted samples is seen, the total area varying from 3.7 to 36.5 square meters. It is also seen that upon gasification there is a marked variation in the increase in surface area for comparable amounts of burn-off. Using the surface area data, the reaction rates can also be expressed in units of grams per hour per square meter at surface. These data are also presented in Table III.

TABLE III
Specific Reaction Rates and Surface Areas Produced for Carbon Samples at Different Temperatures

	Reaction Conditions	Reaction Rate	Total Surface Area	Specific Rate
	°C	gm/hr	m ²	gm/(hr) (m ²)(10 ³)
Graphitized carbon A	Unreacted	—	4.7	—
	900	0.04	24.7	1.6
	1100	1.83	49.5	36.9
Graphitized carbon B	Unreacted	—	3.7	—
	900	0.24	6.0	342
	1100	3.40	9.2	2833
Lampblack	Unreacted	—	27.3	—
	900	0.21	63.8	32.9
	1100	3.00	111.8	26.8
Carbon A	Unreacted	—	36.5	—
	900	0.19	205.6	0.9
	1100	3.98	116.0	34.3
Carbon B	Unreacted	—	5.4	—
	900	0.23	10.9	21.1
	1100	4.04	26.8	150
Carbon C	Unreacted	—	5.0	—
	900	—	5.3	—
	1100	—	14.1	—

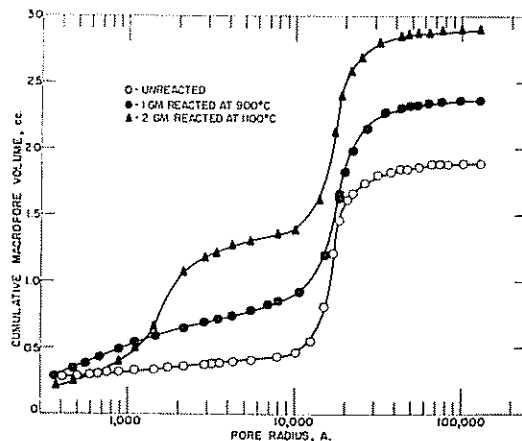


Fig. 5. Change in macropore volume of graphitized carbon A rods upon gasification.

Another technique which has been used successfully to study carbons is mercury porosimetry. Mercury, which has a contact angle with carbon of greater than 90°, is forced into the porous carbon under pressure. By use of the Washburn equation⁴, the volume of mercury forced into carbon is related to pore radius. With the present apparatus, pore volume distributions can be determined over the radius range 350 to 130,000 Å. Figure 5 shows some typical porosimeter data on a graphitized carbon. It is seen that the majority of the pore volume is concentrated in a narrow range of pore radius at about 13,000 Å. This volume is doubtless the void volume between the particles making up the rods. It is further seen that upon gasification the majority of the pore volume is still concentrated in the same pore-radius range but that there is also an increasing amount of pore volume produced in smaller pores.

Figure 6 presents some porosimeter data on lampblack. The important point here is that the majority of the pore volume is now concentrated in pores about 1,000 Å in radius, or a ten-fold shift below that of the graphitized carbon. This is undoubtedly

⁴ H. L. Ritter and C. L. Drake, *Ind. Eng. Chem., Anal. Ed.*, **17**, 782 (1945).

due to the smaller size of the lampblack particles. A second, small concentration of pore volume at a pore radius of 7,000 Å is also noted. Such a distribution of pore volume is indicative of a bimodal distribution of particles.

Another parameter of carbons which is of extreme importance is resistivity. Table IV presents data on the variation of resistivity of a carbon electrode upon burn-off at different temperatures. There are two main points to be observed in this Table. First the change in resistivity at equal burn-offs is a function of the burn-off temperature. Secondly, there is a marked increase in resistivity, up to a ratio of over two, for only 10% burn-off. The very undesirable effect of burn-off with regard to resistivity is, therefore, evident.

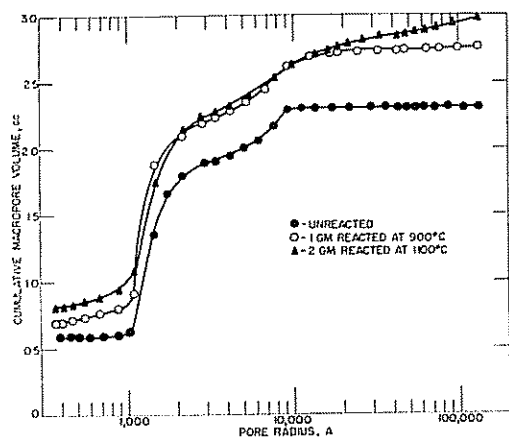


FIG. 6. Change in macropore volume of lampblack rods upon gasification.

TABLE IV
Variation in Resistivity of Carbon Electrodes with Gasification to 10 per cent Weight Loss

Temperature	Resistivity, ohm cm ² /cm	Ratio
	$\times 10^{-4}$	
Unreacted	55	1
900	115	2.09
925	105	1.91
950	85	1.54
1000	100	1.82

TABLE V
Effect of Oxidation at 450°C. on Helium Density of 14 mm. Diameter Graphite Rods*

Per Cent Oxidation	Density, g/cc†	Unavailable Pore Volume, %
None	2.130	6.0
0.55	2.194	3.1
1.70	2.231	1.5
2.70	2.226	1.8

* E. M. Dresel and L. E. J. Roberts, *Nature*, **171**, 170 (1953).

† X-ray diffraction density—2.266 g/cc.

Table V presents data on the variation of helium density of a highly graphitized carbon upon oxidation. First, it is noted that the density calculated from x-ray diffraction data for the graphite is 2.266 gms/cc. On the other hand, the helium density of the original sample is only 2.130 gms/cc, which gives an unavailable pore volume of 6%. Upon oxidation to only 0.55% burn-off, the helium density is increased markedly; and the unavailable pore volume is decreased to 3.1%. Further oxidation to 1.7% burn-off further increases the helium density and decreases the unavailable pore volume. However, it is seen that subsequent oxidation has little additional effect on either helium density or unavailable pore volume. Helium density, in conjunction with x-ray density, is then an excellent technique to measure the change in unavailable pore volume of carbons.

Table VI presents data on the apparent density of carbon rods. The apparent density is, of course, simply determined by either knowing the weight of carbon per unit volume or by displacing a known weight of mercury by a known weight of carbon. Using the apparent and true density data of carbons, the pore volume and porosity of carbons can be determined. These data are also presented in Table VI.

In the study of gas reactions of carbons, one more parameter which is considered of importance is the rate at which the reacting

TABLE VI
Densities and Porosities of Carbons Before and After Gasification

	Reaction Conditions	True Density	Apparent Density	Porosity	Pore Volume
	°C	gm/cc	gm/cc	%	cc/gm
Graphitized carbon A	Unreacted	2.248	1.549	31.1	0.200
	900		1.390	38.2	0.274
	1100		1.189	47.1	0.396
Graphitized carbon B	Unreacted	2.250	1.561	30.6	0.197
	900		1.418	37.0	0.261
	1100		1.280	43.1	0.337
Lampblack	Unreacted	2.168	1.361	37.2	0.274
	900		1.224	43.6	0.356
	1100		1.074	50.5	0.470
Carbon A	Unreacted	2.186	1.579	27.8	0.176
	900		1.438	34.2	0.238
	1100		1.390	36.4	0.262
Carbon B	Unreacted	2.194	1.512	31.1	0.205
	900		1.440	34.4	0.218
	1100		1.312	40.2	0.306
Carbon C	Unreacted	2.192	1.584	27.8	0.175
	900		1.447	34.0	0.235
	1100		1.362	37.9	0.278

gas can diffuse into the pores of the carbon. Particularly at high temperatures this rate of diffusion affects the gasification rate of the carbon and also the uniformity of the gasification reaction through the sample. The higher the gasification temperatures the more uneven the gasification through the rod, with the percentage of gasification on the outside of the sample increasing with increasing temperatures. Figure 7 presents a diagram of the gas-flow apparatus, which is used to determine effective diffusion coefficients for the carbon rods. This apparatus has been designed by the Socony-Mobil Laboratories, who have very kindly been cooperating with us in the diffusion work, and has been described in detail by Weisz and Prater⁵. Hydrogen is flowed at a

high velocity against one face of a $\frac{1}{8}$ inch long by $\frac{1}{8}$ inch diameter carbon sample, fitted tightly within a piece of Tygon tubing; and nitrogen is flowed at a high velocity against the other face of the carbon. The pressure of hydrogen and nitrogen on the two faces is maintained equal. The diffusion coefficient is then determined by analyzing by a thermal conductivity cell for the amount of hydrogen which has diffused

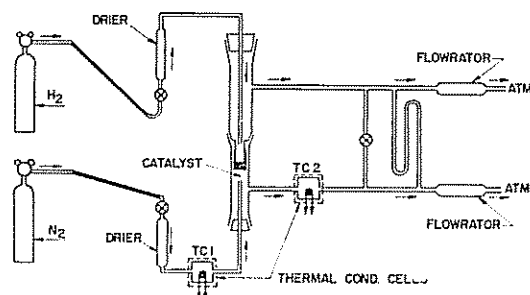


FIG. 7. Diagram of gas flow apparatus

⁵ P. B. Weisz and C. D. Prater, *Advances in Catalysis* (Academic Press, New York, 1954), pp. 187-196.

